

TranSplat: Instant Cross-Scene Object Relighting in Gaussian Splatting via Spherical Harmonic Transfer

Boyang Yu*
Rice University
by12@rice.edu

Yanlin Jin*
Rice University
yj56@rice.edu

Yun He
University of Maryland
yunhe@umd.edu

Akshat Dave
Stony Brook University
dave@cs.stonybrook.edu

Guha Balakrishnan
Rice University
guha@rice.edu

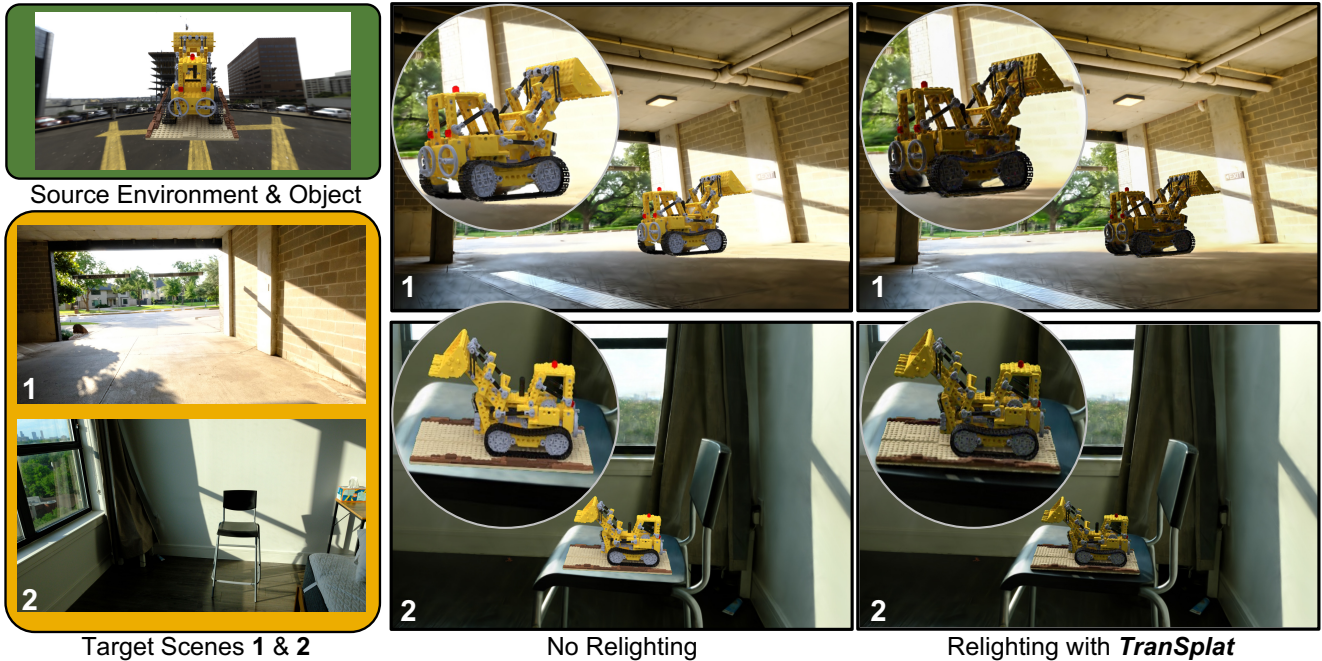


Figure 1. Example demonstrations of *TranSplat* relighting a LEGO bulldozer from a source environment (top left) to target environments (bottom left). We assume that 3D Gaussian Splatting (GS) [18] representations may be built for both the source and target scenes from multiple views (not shown here), and that the object may be extracted (segmented) and placed into the target scene with either automatic or manual supervision. *TranSplat* then relights the object’s Gaussians to reflect appropriate shading and shadow effects for the target environment. Crucially, *TranSplat* requires no ground truth information on the source or target radiance distributions (i.e., environment maps), no decomposition of object materials, and uses lightweight operations taking **10 seconds or less** of processing time.

Abstract

We present *TranSplat*, a method for fast and accurate object relighting for the 3D Gaussian Splatting (GS) framework when transferring a 3D object from a source GS scene to a target GS scene. *TranSplat* is based on a theoretical radiance transfer identity for cross-scene relighting of objects with radially symmetric BRDFs that involves only taking

simple products of spherical harmonic appearance coefficients of the object, source, and target environment maps without any explicit computation of scene quantities (e.g., the BRDFs themselves). *TranSplat* is the first method to demonstrate how this theoretical identity may be used to perform relighting within the GS framework, and furthermore, by automatically inferring unknown source and target environment maps directly from the source and target scene GS representations. We evaluated *TranSplat* on sev-

* Equal contribution.

eral synthetic and real-world scenes and objects, demonstrating comparable 3D object relighting performance to recent conventional inverse rendering-based GS methods with a fraction of their runtime. While *TranSplat* is theoretically best-suited for radially symmetric BRDFs, results demonstrate that *TranSplat* still offers perceptually realistic renderings on real scenes and opens a valuable, lightweight path forward to relighting with the GS framework.

1. Introduction

The 3D Gaussian Splatting (GS) framework has demonstrated remarkable power and computational speed for high-quality, real-time neural rendering applications [18]. An important next frontier for GS is enabling realistic 3D scene editing and composition applications. This study focuses on one such task, *cross-scene object relighting*. In this task, we assume that a set of input views of two scenes, the *source* and *target*, are given, along with 2D masks specifying an object of interest in the source views. After automatically extracting the 3D object from the source model and placing it in the target scene with manual input, the goal is to relight the object appropriately to agree with the target scene’s environment (see Fig. 1 and Fig. 8). The key challenge of this task is that the object’s perceived illumination must change as a function of both the target and source scene’s radiance distributions (i.e., environment maps), which are unknown.

This study introduces *TranSplat*, a method to instantly and realistically relight an object transferred from source to target GS scenes (i.e., within seconds on a single A6000 GPU). To do so, we take inspiration from a theoretical identity relating the spherical harmonic (SH) coefficients of surfaces with radially symmetric BRDFs (e.g., Lambertian or Phong) under different lighting conditions [24]. The key result of this identity is that relighting an object with such a surface may be approximated by simply multiplying its SH appearance coefficients by the ratios of target and source environment map SH coefficients (see Eq. 6). Crucially, this *radiance transfer* procedure bypasses explicit inverse rendering estimation of quantities such as bidirectional reflectance distribution functions (BRDFs), trading off some modeling complexity for a significant improvement in runtime. *TranSplat* is the first method to show how this theoretical radiance transfer operation may be used to perform fast and accurate relighting within the GS framework.

More specifically, we first fit GS models to the source and target scenes and extract the object of interest from the source scene by propagating 2D masks to 3D. After a user manually inserts the object into the target scene at an appropriate location, *TranSplat* performs its core function: fast and realistic object relighting. *TranSplat* samples spatially varying source and target environment maps directly from the trained GS representations with a novel cube map sam-

pling strategy centered at the object’s location. *TranSplat* then relights the object using source and target environment maps by applying the identity described above to the SH appearance coefficients of each of the object’s Gaussians. We further use the sampled target environment maps to infer and add appropriate shadows to the object and its surroundings in a postprocessing step by attenuating Gaussian SH appearance coefficients. The entire framework is carried out as a single lightweight analytical computation that does not require any iterative inverse rendering optimization.

This work is related to several relighting methods proposed in the past two years for GS [13, 14, 22], but differs in two key aspects. First, prior methods typically perform scene-level relighting, approximating the illumination as a fixed 2D HDR environment map placed far from the scene. This representation remains constant even if an inserted object is moved within the scene, and therefore cannot capture spatial variation in lighting. In contrast, *TranSplat* leverages the 3DGS radiance field to infer spatially varying source and target environment maps centered at the object’s location. Second, all of these methods rely on traditional inverse-rendering pipelines requiring explicit, per-scene disentanglement and estimation of complex material and lighting properties (e.g., BRDFs) from input images. While offering higher scene-modeling flexibility than *TranSplat*, these methods require slow, iterative per-scene optimization to solve an inherently ill-posed estimation problem [4]. In contrast, the approximate yet lightweight spherical harmonic transfer formulation allows *TranSplat* to perform instant relighting.

We first quantitatively evaluated *TranSplat* on a custom blender synthetic dataset and the TensoIR dataset [15]. *TranSplat* delivers competitive or better relighting accuracy compared to baseline GS [14, 20, 22, 30] and diffusion-based [16] methods, while being orders of magnitude faster. We then further qualitatively demonstrate *TranSplat*’s cross-scene object relighting results on a series of real-world scenes with different environment lighting from our own captures.

2. Related work

Our work is related to the broad field of inverse rendering – the estimation of physical scene properties such as lighting, surface normals, and materials from images – but differs fundamentally in that it bypasses explicit inverse estimation to perform relighting. Classical inverse rendering techniques relied on iterative optimizations using physics, geometry, and signal processing cues [5, 10, 11, 24, 25, 28]. Due to the ill-posedness of the task, they typically focused on controlled setups and/or a priori known scene properties.

The first inverse rendering methods using deep learning relied on typical feed-forward networks trained over large labeled datasets to predict attributes such as color, shape,

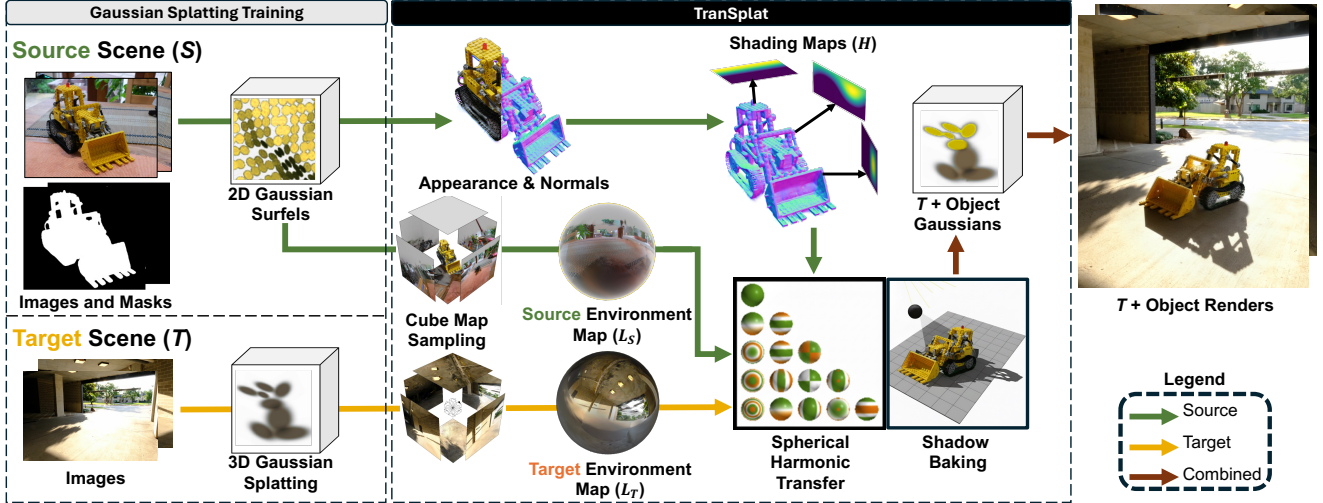


Figure 2. **Overview of *TranSplat*.** Given source and target scenes, *TranSplat* first fits a Gaussian Surfels [9] model to the source scene (S) using input images and object masks, and a standard 3D Gaussian Splatting model to the target scene (T). From each trained GS representation, *TranSplat* renders cube maps centered at the object’s location to estimate spatially varying environment maps (L_S , L_T). Using these environment maps and per-Gaussian normals, *TranSplat* performs *Spherical Harmonic Transfer*, an analytical transformation function applied on each Gaussian’s spherical harmonic (SH) appearance coefficients by the ratio of target to source lighting coefficients, modulated by per-Gaussian shading maps (H). Finally, a lightweight shadow-baking step uses the dominant light lobes of L_T to generate spatially consistent shadows, and the merged model is rendered to produce novel target-scene views.

and other material properties [21, 31, 36]. Neural radiance fields (NeRFs) [1, 2, 27] spawned a paradigm shift in inverse rendering, relying on a per-scene optimization driven by a multilayer perceptron (MLP) scene encoding and rendering objective. Following methods such as Nerf-in-the-Wild [26] and NeRD [6] demonstrated that “transient” lighting effects may be separated from constant scene properties from image collections. Several NeRF-derived methods explore deeper integration of physically-based rendering techniques with MLPs to disentangle object-specific and lighting properties [32, 35, 37, 38]. Tensorial Inverse Rendering (TensoIR) further combines MLPs with tensor factorization to yield a representation with lower computational cost and facilitating second-bounce ray marching [15]. Other hybrid methods, such as Neural-PBIR [34], combine neural scene representations with traditional physics-based inverse rendering (PBIR) in a multi-stage pipeline to achieve high-fidelity material and lighting refinement.

Several recent inverse rendering and relighting methods now build on the 3D Gaussian Splatting (GS) [18] framework, and operate using physically-based rendering to estimate surface properties for each Gaussian in a scene [13, 14, 22, 30]. When relying solely on single-environment captures, these methods often struggle to disentangle lighting from material properties. To address this ambiguity, some works propose data-level solutions. ReCap [20], for instance, leverages cross-environment captures to enforce a consistent material estimation across multiple lighting con-

ditions. A distinct class of relighting methods similarly bypasses the 3DGS-IR problem by leveraging generative diffusion priors. IllumiNeRF [39] and Neural Gaffer [16] both adopt a two-stage strategy: they first perform diffusion-based 2D image-space relighting conditioned on an environment map, then distill the results into a 3D NeRF representation. While this paradigm removes the need for explicit geometry or material estimation, it comes with practical drawbacks—IllumiNeRF requires slow multi-view diffusion inference and full NeRF retraining for each relit scene, and Neural Gaffer’s outputs remain limited to low-resolution (256×256) renderings and lack geometric consistency across views. In contrast, *TranSplat* leverages a theoretical radiance transfer identity in 2D based on spherical harmonics [24] (described in Sec. 3.1), yielding a lightweight post-processing directly modulating the SH coefficients of a pre-trained Gaussian splatting representation and avoiding material property estimation, generative priors, and costly retraining.

3. Methods

TranSplat takes images and corresponding 2D object masks of a source scene as input, along with a pretrained 3DGS model of a target scene. After extracting a Gaussian Surfels model of the object from the source scene, *TranSplat*’s goal is to perform instant relighting under target illumination conditions. To accomplish this, *TranSplat* estimates the source and target environment maps L_S and L_T , and per-

forms lighting transfer by rescaling the spherical harmonic (SH) coefficients of the object’s surfels based on the ratio of SH coefficients between L_T and L_S . This formulation enables physically consistent and spatially accurate relighting with minimal computational overhead. The complete workflow of *TranSplat* is illustrated in Fig. 2.

3.1. Radiance Transfer Background

We build on a theoretical framework for radiance transfer with spherical harmonics (SHs), originally presented for 2D images only, that obviates the need to estimate bidirectional reflectance distribution functions (BRDFs) assumed to be radially symmetric (e.g., Lambertian) [24]. Consider a point \mathbf{x} on a 3D surface with surface normal $\mathbf{n} = (\alpha, \beta)$, and radially symmetric BRDF $\rho(\theta)$. The rendering equation [17] states:

$$B(\mathbf{n}) = \int_{\Omega} \rho(\theta) L(\omega) \max(\mathbf{n} \cdot \omega, 0) d\omega, \quad (1)$$

where $B(\mathbf{n})$ is the outgoing radiance at \mathbf{x} , $L(\omega)$ is the incoming radiance from direction $\omega = (\theta, \phi)$, and Ω represents the hemisphere above the point \mathbf{x} . Using spherical harmonic bases $Y_{lm}(\theta, \phi)$, we obtain the following:

$$L(\theta, \phi) = \sum_{l=0}^L \sum_{m=-l}^l L_{lm} Y_{lm}(\theta, \phi), \quad (2)$$

$$B(\alpha, \beta) = \sum_{l=0}^L \sum_{m=-l}^l B_{lm} Y_{lm}(\alpha, \beta), \quad (3)$$

$$\rho(\theta) = \sum_{l=0}^L \rho_l Y_{l0}(\theta). \quad (4)$$

It can be shown that in the frequency domain, each coefficient B_{lm} is given by a simple product formula [3, 28]:

$$B_{lm} = A_l L_{lm}, \quad (5)$$

where $A_l = \sqrt{4\pi/(2l+1)}\rho_l$. Assuming A_l is constant for the object across scenes, we obtain the following relation when imaging the surface in two environments S and T :

$$\frac{B_{lm}^T}{B_{lm}^S} = \frac{L_{lm}^T}{L_{lm}^S} = H_{lm} \implies B_{lm}^T = B_{lm}^S H_{lm}, \quad (6)$$

where H_{lm} is referred to as the *lighting transfer function*.

3.2. GS Model Fitting

While the radiance transfer formulation used in *TranSplat* is agnostic to the specific Gaussian splatting variant used to represent objects, we choose to use the Gaussian Surfels [9] framework. We adopt surfels instead of the original 3D Gaussian ellipsoids [18] because they provide better explicit surface normals with their flat structure, useful in our relighting procedure (Sec. 3.4). We assume that the target scene is simply fit with the original 3DGS (ellipsoid) model.

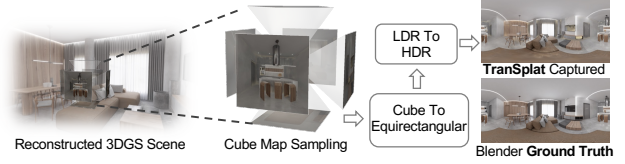


Figure 3. **Capture an explicit environment map directly from 3D Gaussian fields.** We render six 90° views around a specified position to obtain a cubemap, which is then converted into an equirectangular environment map. The position corresponds to the object’s original location to sample the source lighting or the target location where the object will be inserted.

3.3. Lighting Estimation

The incident illumination radiances $L_S(\theta, \phi)$ and $L_T(\theta, \phi)$ are needed to perform relighting and typically represented as environment maps. If environment maps are unknown, we propose a strategy to estimate their spherical harmonic (SH) coefficients directly from trained GS scene representations, as illustrated in Fig. 3.

Specifically, we first render the incoming radiance from six orthogonal viewing angles forming the six faces of a cubemap. We sample the cubemap at the position center of the scene or the target location where the Gaussian object will be inserted in the new environment. We then create an equirectangular environment map by linking each spherical coordinate to a cubemap face, and sampling the corresponding pixel value. We convert the resulting low-dynamic-range (LDR) map to HDR using an off-the-shelf LDR-to-HDR model [23]. Finally, to account for possible differences in coordinate frames, such as those caused by object rotation or scene alignment, we apply a corresponding rotation to S ’s environment map. Details on environment map construction are in Supplementary.

3.4. Cross-Scene Relighting with Shading Maps

TranSplat applies relighting factors to ensure the represented objects exhibit a natural appearance under illumination L_T . To do so, we extend the relation in Eq. 6 to GS. In particular, unlike the 2D case studied by Mahajan et al. [24], each element of the 3D environment maps $L_S(\theta, \phi)$ and $L_T(\theta, \phi)$ will not equally affect the appearance of every Gaussian in a GS model. In fact, for solid objects, we would expect an object’s Gaussians to occlude one another from different portions of the environment lighting. The impact of each point in the environment on a Gaussian must be modulated by the degree to which that Gaussian faces that point (see Fig. 4). To that end, for Gaussian j with normal vector \mathbf{n}^j , we compute a modulated environment map:

$$L_S^j(\theta, \phi) = L_S(\theta, \phi) \cdot H^j(\theta, \phi), \quad (7)$$

where $\mathbf{u}_{\theta, \phi}$ is the unit vector oriented at (θ, ϕ) , and $H^j(\theta, \phi) = \max\{\mathbf{n}^j \cdot \mathbf{u}_{\theta, \phi}, 0\}$ is a *shading map*. We per-

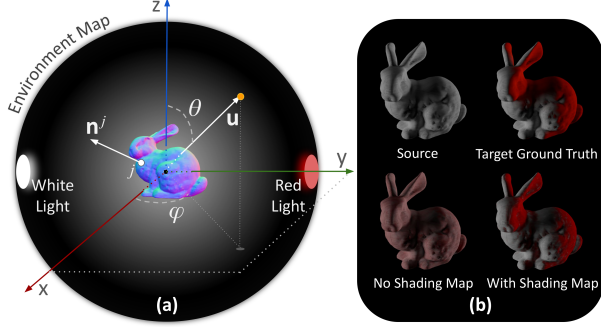


Figure 4. **Conceptual schematic of the shading map computation for a simple scene.** (a) The shading map measures the contribution of each point in an environment map on each Gaussian surfel j of the object (here, a bunny). The contribution is based on the angular alignment of the surfel’s normal \mathbf{n}^j with the point. In this example, Gaussian j would not be strongly affected by the point along \mathbf{u} with orientation (θ, ϕ) . (b) Without applying the shading map, all Gaussians receive input from all environment map points, resulting in a uniform appearance, whereas with shading, accurate colors and shadows are rendered.

form the analogous computation to produce $L_T^j(\theta, \phi)$, and arrive at the lighting transfer function for Gaussian j (in SH coefficients):

$$\tau_{lm}^j = L_{T,lm}^j / (L_{S,lm}^j + \varepsilon), \quad (8)$$

where ε is a small constant. In practice, τ_{lm}^j can become unstable when any source coefficient $L_{S,lm}^j$ is close to zero, which may occur under degenerate or highly saturated lighting conditions (e.g., a near-monochromatic environment). We address this by clamping τ_{lm}^j to a bounded range.

3.5. Shadows

Finally, to enhance cross-scene relighting realism, we implement a lightweight shadow module that produces physically plausible shadows consistent with the target lighting L_T . We extract the K dominant light lobes by smoothing L_T with a low-order spherical-harmonic kernel to obtain a stable intensity field, then detect its brightest angular directions as dominant illumination lobes. For each lobe, we treat the object’s Gaussians as soft occluders and orthographically project them onto a receiver plane to generate a per-lobe shadow transmittance map. This map is baked into background Gaussians or used to modulate the spherical-harmonic coefficients of receiver Gaussians during shading. All K maps are composited to form the final soft shadow. As shown in Fig. 6, since dominant lobes are re-evaluated whenever the environment map changes (e.g., under rotation), shadows update dynamically and stay consistent with both the object and target illumination. We emphasize that this shadow module is a lightweight post-processing step

solely to improve perceptual realism, not a core contribution of our method.

4. Experiments

We evaluate *TranSplat* in terms of relighting accuracy, efficiency, and cross-scene object insertion, using images and objects from MipNeRF360 [2], TensorIR-Synthetic [15], Toys4K [33], as well as our own captured scenes which have more directional light sources. Experiments measure qualitative and quantitative relighting fidelity and run-time efficiency; details follow in the subsections below.

4.1. Relighting Accuracy

We compare *TranSplat* against five baseline algorithms (GS-IR [22], R3DG [13], Recap [20], GaussianShader [14], and Neural Gaffer [16]) on the task of relighting. We use five objects (*Armadillo*, *Lego*, *Ficus*, *Dragon*, *Tower*) and HDR maps commonly used by prior works. The ground truths for *Dragon* and *Tower* are obtained in Blender. For a consistent comparison, we use the same source environment (*City*) for all cases. We present numerical results in Table 1, and visual results in Fig. 7. In general, *TranSplat*’s relight renders are closest to ground truth. All methods are able to relight the object to the correct color tone, but the results from the GaussianShader [14] appear noticeably brighter. Neural Gaffer [16] produces accurate shading and shadows, but its outputs are limited to 256×256 pixels due to its resolution constraint. Our method achieves the highest PSNR on all cases except *Ficus*, mainly because the ficus pot surface is not sufficiently Lambertian. Fig. 5 shows relighting results of the same object (owl) under more directional lighting, also demonstrating relighting in both directions between the city and sunset environments.

4.2. Relighting Efficiency Comparison

Table 2 compares the per-scene runtime of all methods. For inverse-rendering-based methods such as Recap and GaussianShader, lighting-related properties are optimized during training, so their training and relighting times are considered jointly. *TranSplat* is significantly faster than all baseline methods. Once the surfel representation is trained, it only takes a few seconds to adapt the Gaussian object color, since our approach is purely analytical rather than optimization- or learning-based.

4.3. Cross-Scene Object Transfer

TranSplat is a training-free and efficient relighting framework that directly adapts the colors of pre-trained Gaussians to novel lighting conditions. One typical application, which corresponds to a fundamental task in rendering engines, lies in inserting 3D Gaussian object assets into novel scenes. This usually requires object segmentation and spatial place-

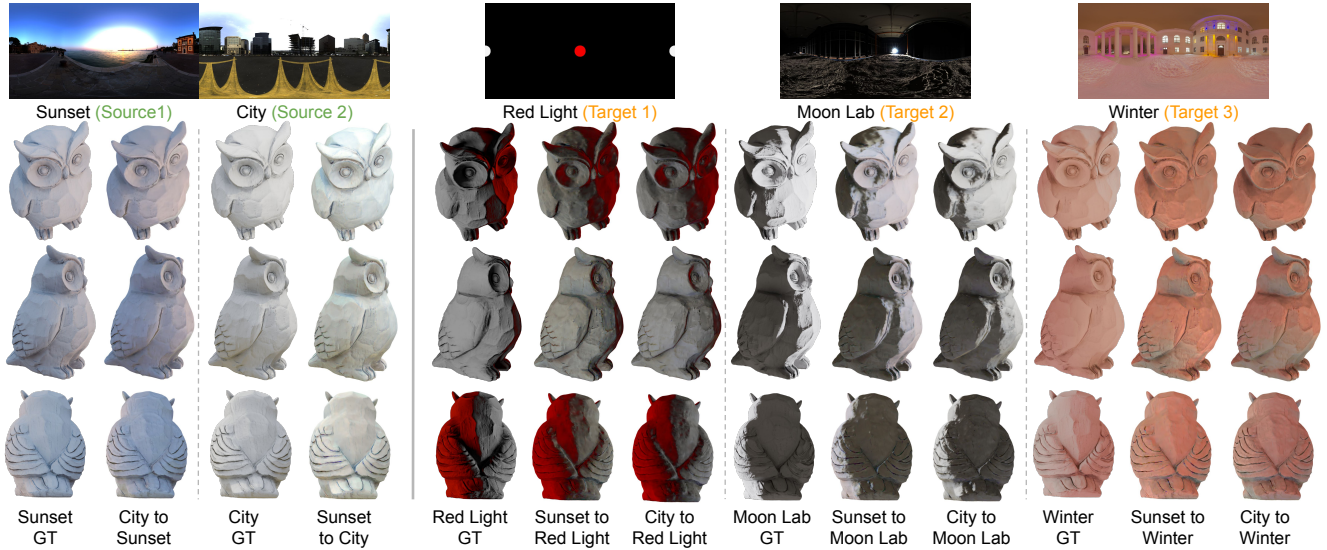


Figure 5. **Relighting results of *TransPlat* across various environments.** We use city and sunset environments as the source lighting conditions. In addition to three target environment with distinct color tones and directional lighting, we also include, in the left four columns, the results of swapping the city and sunset lighting conditions. *TransPlat* produces relighting results that closely match the GT shading and color tone.

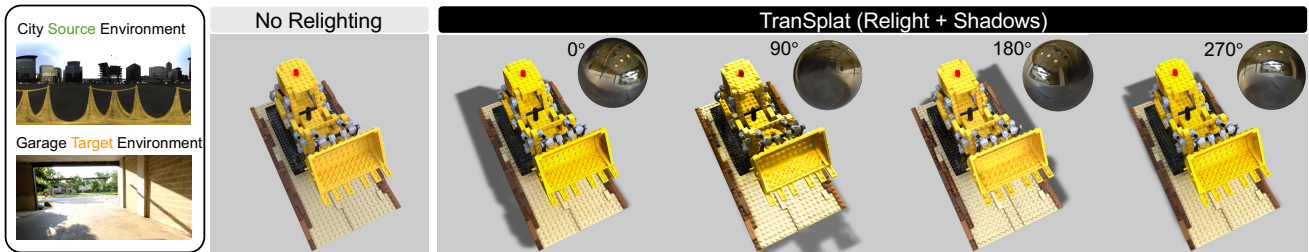


Figure 6. **Demonstration of Spatially-Variant Relighting and Dynamic Shadows (Sec. 3.4 & 3.5).** (Left) The source object under ‘City’ lighting environment map. (Right) The object is relit using the ‘Garage’ environment map. Our method uses per-Gaussian **shading maps** (Sec. 3.4) to ensure the object’s appearance correctly responds to the lighting’s spatial directionality. Our shadow module (Sec. 3.5) derives its casting direction from the *same* envmap. As the environment map is rotated (90°, 180°, 270°), the cast shadows dynamically adapt, demonstrating that both relighting and shadows are consistently driven by the same spatially-variant illumination source.

Table 1. **Quantitative evaluation of relighting methods.** We compare *TransPlat* against GS-IR [22], GaussianShader, R3DGS, Recap, and Neural Gaffer on three environment maps (fireplace, forest, sunset). The best results are highlighted in green, second-best in orange.

	fireplace					forest					sunset							
	GS-IR	GShader	R3DGS	Recap	Neural Gaffer	<i>TransPlat</i>	GS-IR	GShader	R3DGS	Recap	Neural Gaffer	<i>TransPlat</i>	GS-IR	GShader	R3DGS	Recap	Neural Gaffer	<i>TransPlat</i>
PSNR (dB) ↑																		
lego	24.0	13.12	23.44	19.65	23.76	30.7	22.5	13.64	26.66	23.89	23.80	27.2	23.6	12.82	25.97	22.83	23.69	30.6
armadillo	28.0	23.05	27.66	32.35	30.09	32.37	27.3	21.75	26.37	31.50	29.05	34.8	27.7	20.14	25.99	30.94	28.79	34.2
dragon	23.96	15.96	23.81	24.92	23.29	26.54	20.86	16.08	24.48	25.42	26.69	25.70	22.66	15.55	23.20	23.98	27.08	27.74
figus	29.9	25.76	25.07	27.44	24.38	25.2	27.5	22.61	27.17	30.10	25.39	27.8	28.2	22.13	28.41	29.92	26.05	27.4
tower	22.39	13.92	22.40	24.66	25.13	25.28	18.46	13.77	24.11	23.80	26.58	24.33	20.14	13.78	25.10	23.97	27.09	27.67
SSIM ↑																		
lego	0.86	0.76	0.83	0.83	0.84	0.95	0.86	0.82	0.93	0.92	0.85	0.87	0.89	0.81	0.92	0.91	0.84	0.94
armadillo	0.92	0.97	0.90	0.92	0.95	0.94	0.93	0.92	0.95	0.97	0.95	0.97	0.94	0.91	0.96	0.97	0.96	0.97
dragon	0.87	0.83	0.87	0.89	0.87	0.89	0.87	0.87	0.94	0.95	0.92	0.94	0.90	0.87	0.94	0.95	0.92	0.95
figus	0.97	0.95	0.95	0.97	0.95	0.96	0.96	0.94	0.97	0.98	0.95	0.97	0.97	0.94	0.97	0.98	0.95	0.97
tower	0.86	0.82	0.85	0.89	0.88	0.87	0.84	0.82	0.90	0.95	0.95	0.91	0.89	0.85	0.93	0.96	0.96	0.94
LPIS ↓																		
lego	0.10	0.14	0.12	0.10	0.16	0.05	0.09	0.12	0.05	0.06	0.17	0.10	0.09	0.13	0.06	0.06	0.17	0.05
armadillo	0.07	0.05	0.07	0.06	0.08	0.05	0.06	0.07	0.07	0.06	0.07	0.05	0.06	0.07	0.05	0.04	0.08	0.05
dragon	0.10	0.13	0.10	0.07	0.08	0.08	0.09	0.10	0.06	0.05	0.11	0.06	0.09	0.11	0.06	0.05	0.11	0.05
figus	0.03	0.04	0.04	0.03	0.06	0.04	0.04	0.05	0.03	0.02	0.03	0.03	0.04	0.05	0.03	0.02	0.03	0.03
tower	0.09	0.11	0.12	0.06	0.06	0.10	0.10	0.13	0.08	0.04	0.03	0.08	0.09	0.14	0.09	0.04	0.03	0.07

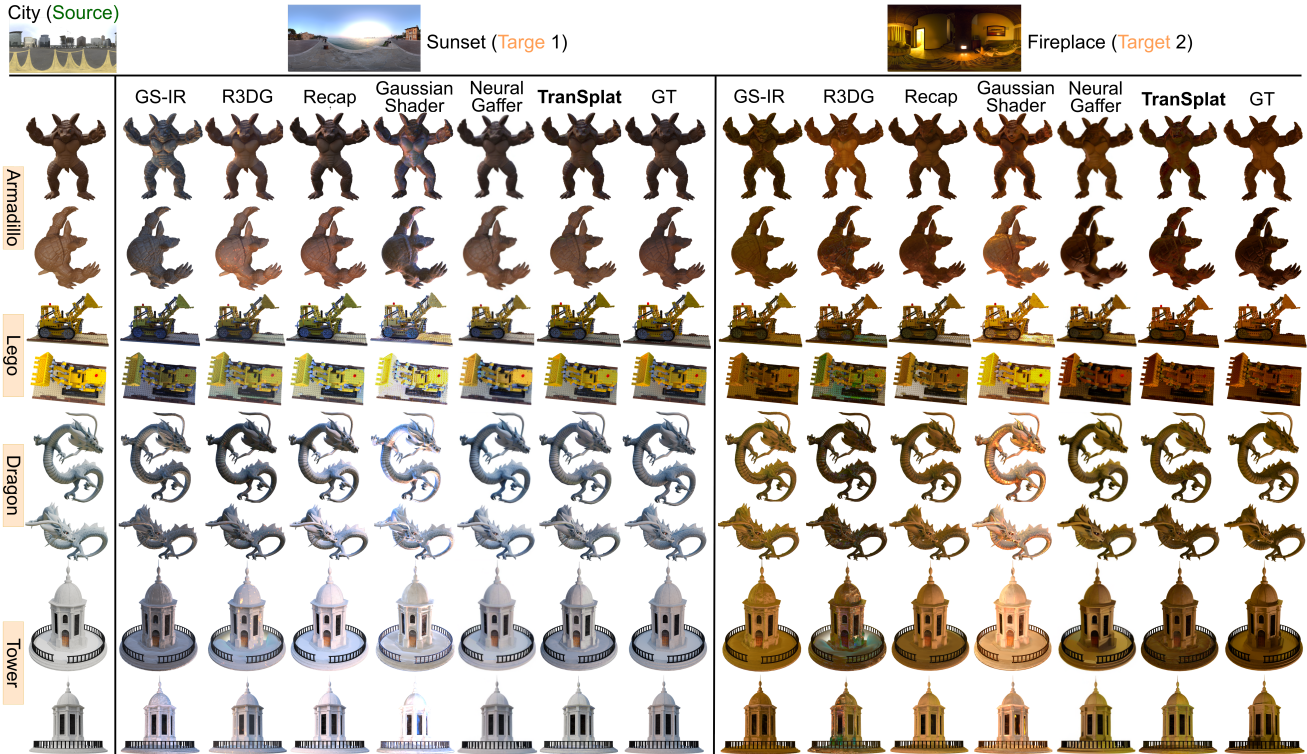


Figure 7. **Relighting results using two Blender-generated (Dragon [33] and Tower) and two TensoIR [15] objects.** We apply the same (HDR) source environment map (*City*) to all objects, and then relight them to three other environment maps: *Sunset*, *Fireplace*, and *Forest*. We recommend zooming in to inspect fine-grained shading detail. *TranSplat* achieves the best visual quality in terms of color and shading effects compared to ground truth (GT). See Table 1 for corresponding metrics.

Table 2. **Training and relighting efficiency.** Average per-scene runtimes measured on a single A6000 GPU. *Scene reconstruction* denotes the time required for 3D scene modeling, such as initial 3DGS or Gaussian Surfels training, while *relighting optimization* refers to the time each method takes to train or optimize the model for relighting the reconstructed object through processes such as material decomposition [13, 15, 22], spherical harmonic modulation in *TranSplat*, or diffusion-based training [16]. In comparison, *TranSplat* achieves instant relighting, completing the full process in a fraction of the time required by all other methods.

	GS-IR	GaussianShader	Relightable 3DGS	Recap	Neural Gaffer	<i>TranSplat (Ours)</i>
Scene Modeling Time	16 min	97 min	16 min	60 min	17 min	10 min
Relighting Optimization Time	47 min		84 min		57600 min	0.1 min
Total Time per Scene	63 min	97 min	100 min	60 min	57617 min	10.1 min

ment, followed by relighting to achieve visually consistent integration with the target environment.

To demonstrate that *TranSplat* relights the objects consistently with the illumination of the scene, we recorded four scenes with lighting conditions that differ significantly from the source, particularly those with strong directional light. The inserted objects are *Lego*, *ficus* from TensoIR [15], two blender objects (*Bunny* and *Tower*). Note that the *Lego* object in the first row is extracted from the *MipNeRF* [2] kitchen source GS scene with our segmentation method (see Supplementary). Segmented objects will require additional sampling of the source map at their orig-

inal position in S . We noticed that for some scenes, the sampled environment can contain missing regions due to unobserved areas in the dataset, such as the sky or ceiling. To address this, we adjusted the GS-rendered background to better match the colors of the walls or the sky.

We compare objects inserted using *TranSplat* before and after relighting in Fig. 8. Directly inserting objects into T often results in unrealistic lighting appearances. For example, the *ficus* from TensoIR [15] appears overly bright in a nighttime scene. Beyond general brightness differences, realistic shading effects also emerged. For instance, in the second row, the bunny and tower appear brighter on the side

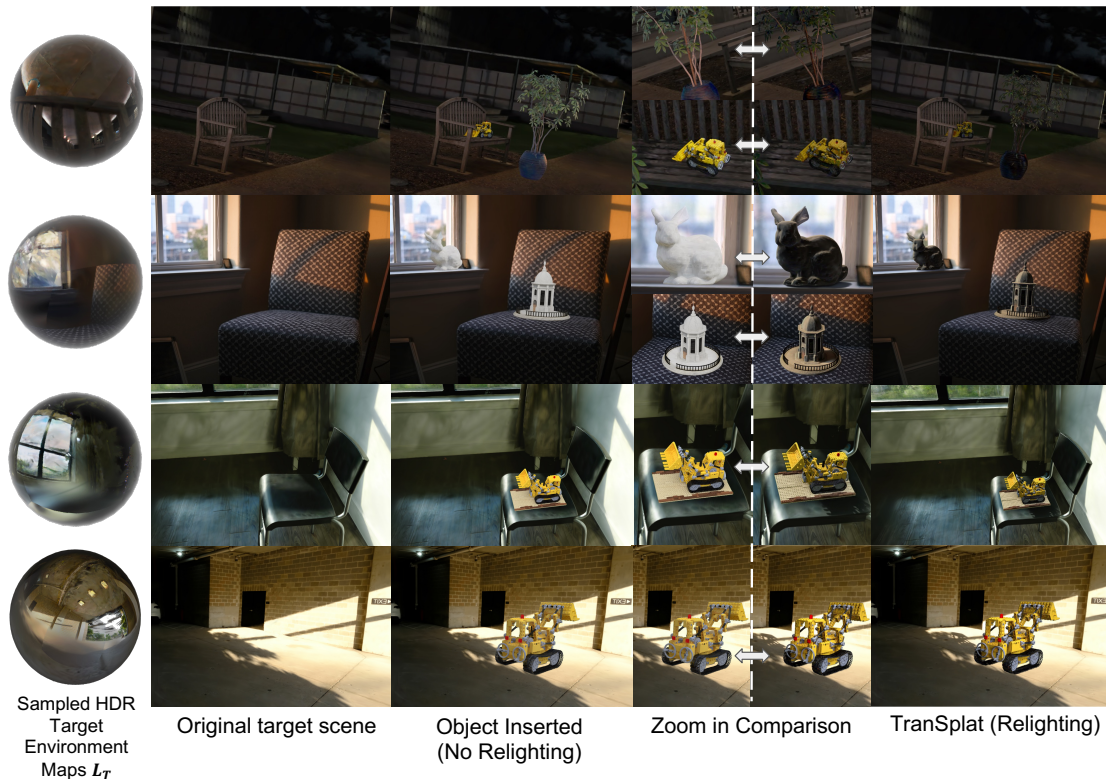


Figure 8. **Sample results demonstrating *TranSplat*'s ability at object transfer into real scenes.** Injecting objects into another scene without relighting renders incongruous appearances with unnatural color and illumination, yet with the addition of *TranSplat*'s relighting optimization, renderings appear more natural. Details are best observed in Supplementary videos.

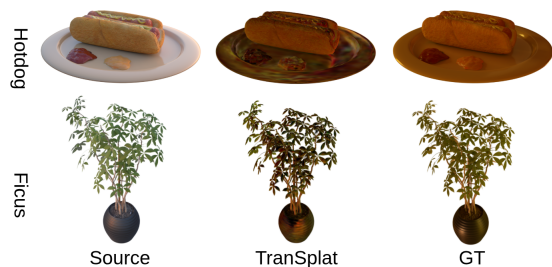


Figure 9. **Failure cases due to non-Lambertian effects.** We present relighting results using *TranSplat* on two objects from the TensoIR [15], relit from the *City* source environment to *Fireplace* target. For non-specular regions such as the hotdog and branches of the Ficus, *TranSplat* deliver reasonable color tones. However, *TranSplat* fails to recover accurate colors for specular regions such as the plate and sauces near the hotdog, and the ficus pot.

facing the window, and the Lego bulldozer in the third row takes on a darker tone on the side facing the camera.

5. Discussion and Limitations

The results demonstrate that *TranSplat*'s cross-environment relighting is on par with or better than other state-of-the-

art neural relighting baselines in accuracy, and markedly more efficient. Instead of spending time decomposing Gaussian material properties, *TranSplat*, as a post relighting framework, directly performs fast numerical computation on Spherical Harmonics coefficients using information from the source and target lighting. Combined with our proposed normal-based shading map, GS environment map sampling, and post-shadowing, we further achieve more realistic insertion of GS objects into real scenes.

TranSplat does have some limitations. First, since *TranSplat* relies on radiance transfer ratios, numerical issues can arise when the source environment lacks energy in some channels as division by zero will lead to instabilities. Second, *TranSplat*'s model of light rendering is simplistic. It assumes that the object has a radially symmetric BRDF, and does not explicitly take into account non-global lighting effects, such as inter-object reflections. This is different from algorithms based on physically-based rendering models that can capture these complexities. Fig. 9 presents two cases where *TranSplat*'s relighting results are not satisfactory due to these assumptions not holding. Third, although *TranSplat* does not require any additional material or BRDF estimation, its performance is highly dependent on the accuracy of Gaussian surfel normals, which directly

affect the shading map computation. Consequently, scenes with complex indoor geometry or weak normal estimates remain challenging for consistent relighting. Nevertheless, *TransSplat* maintains extremely fast relighting in indoor scenes and achieves quality comparable to state-of-the-art inverse-rendering-based Gaussian relighting methods. As our focus is on object-level relighting, detailed indoor results and comparisons are provided in the Appendix. Future work includes improving normal estimation and extending *TransSplat* to more challenging relighting scenarios.

Acknowledgments

This research is based upon work supported by the Office of the Director of National Intelligence (ODNI), Intelligence Advanced Research Projects Activity (IARPA), via IARPA R&D Contract No. 140D0423C0076. The views and conclusions contained herein are those of the authors and should not be interpreted as necessarily representing the official policies or endorsements, either expressed or implied, of the ODNI, IARPA, or the U.S. Government. The U.S. Government is authorized to reproduce and distribute reprints for Governmental purposes notwithstanding any copyright annotation thereon.

References

- [1] Jonathan T Barron, Ben Mildenhall, Matthew Tancik, Peter Hedman, Ricardo Martin-Brualla, and Pratul P Srinivasan. Mip-nerf: A multiscale representation for anti-aliasing neural radiance fields. In *Proceedings of the IEEE/CVF International Conference on Computer Vision*, pages 5855–5864, 2021. 3
- [2] Jonathan T. Barron, Ben Mildenhall, Dor Verbin, Pratul P. Srinivasan, and Peter Hedman. Mip-nerf 360: Unbounded anti-aliased neural radiance fields. 2022. 3, 5, 7, 1, 2
- [3] Ronen Basri and David W Jacobs. Lambertian reflectance and linear subspaces. *IEEE transactions on pattern analysis and machine intelligence*, 25(2):218–233, 2003. 4
- [4] Jeremy Birn. *Digital lighting & rendering*. Pearson Education, 2014. 2
- [5] Samuel Boivin and André Galalowicz. Image-based rendering of diffuse, specular and glossy surfaces from a single image. In *Proceedings of the 28th annual conference on Computer graphics and interactive techniques*, pages 107–116, 2001. 2
- [6] Mark Boss, Raphael Braun, Varun Jampani, Jonathan T Barron, Ce Liu, and Hendrik Lensch. Nerf: Neural reflectance decomposition from image collections. In *Proceedings of the IEEE/CVF International Conference on Computer Vision*, pages 12684–12694, 2021. 3
- [7] Jiazhong Cen, Jiemin Fang, Chen Yang, Lingxi Xie, Xiaopeng Zhang, Wei Shen, and Qi Tian. Segment any 3d gaussians. *arXiv preprint arXiv:2312.00860*, 2023. 2
- [8] Yiwen Chen, Zilong Chen, Chi Zhang, Feng Wang, Xiaofeng Yang, Yikai Wang, Zhongang Cai, Lei Yang, Huaping Liu, and Guosheng Lin. Gaussianeditor: Swift and controllable 3d editing with gaussian splatting. In *Proceedings of the IEEE/CVF conference on computer vision and pattern recognition*, pages 21476–21485, 2024. 1, 2
- [9] Pinxuan Dai, Jiamin Xu, Wenxiang Xie, Xinguo Liu, Huamin Wang, and Weiwei Xu. High-quality surface reconstruction using gaussian surfels. In *ACM SIGGRAPH 2024 Conference Papers*. Association for Computing Machinery, 2024. 3, 4, 1, 2
- [10] Paul Debevec, Chris Tchou, Andrew Gardner, Tim Hawkins, Charis Poullis, Jessi Stumpfel, Andrew Jones, Nathaniel Yun, Per Einarsson, Therese Lundgren, et al. Estimating surface reflectance properties of a complex scene under captured natural illumination. *Conditionally Accepted to ACM Transactions on Graphics*, 19:2, 2004. 2
- [11] Frédo Durand, Nicolas Holzschuch, Cyril Soler, Eric Chan, and François X Sillion. A frequency analysis of light transport. *ACM Transactions on Graphics (TOG)*, 24(3):1115–1126, 2005. 2
- [12] Ainaz Eftekhari, Alexander Sax, Jitendra Malik, and Amir Zamir. Omnidata: A scalable pipeline for making multi-task mid-level vision datasets from 3d scans. In *Proceedings of the IEEE/CVF International Conference on Computer Vision*, pages 10786–10796, 2021. 1, 3
- [13] Jian Gao, Chun Gu, Youtian Lin, Hao Zhu, Xun Cao, Li Zhang, and Yao Yao. Relightable 3d gaussian: Real-time point cloud relighting with brdf decomposition and ray tracing. *arXiv:2311.16043*, 2023. 2, 3, 5, 7
- [14] Yingwenqi Jiang, Jiadong Tu, Yuan Liu, Xifeng Gao, Xiaoxiao Long, Wenping Wang, and Yuexin Ma. Gaussian-shader: 3d gaussian splatting with shading functions for reflective surfaces. In *Proceedings of the IEEE/CVF Conference on Computer Vision and Pattern Recognition*, pages 5322–5332, 2024. 2, 3, 5
- [15] Haian Jin, Isabella Liu, Peijia Xu, Xiaoshuai Zhang, Songfang Han, Sai Bi, Xiaowei Zhou, Zexiang Xu, and Hao Su. Tensor: Tensorial inverse rendering. In *Proceedings of the IEEE/CVF Conference on Computer Vision and Pattern Recognition (CVPR)*, 2023. 2, 3, 5, 7, 8
- [16] Haian Jin, Yuan Li, Fujun Luan, Yuanbo Xiangli, Sai Bi, Kai Zhang, Zexiang Xu, Jin Sun, and Noah Snavely. Neural gaffer: Relighting any object via diffusion. In *Advances in Neural Information Processing Systems*, 2024. 2, 3, 5, 7
- [17] James T. Kajiya. The rendering equation. page 4, 1986. 4
- [18] Bernhard Kerbl, Georgios Kopanas, Thomas Leimkühler, and George Drettakis. 3d gaussian splatting for real-time radiance field rendering. *ACM Transactions on Graphics*, 42(4), 2023. 1, 2, 3, 4
- [19] Alexander Kirillov, Eric Mintun, Nikhila Ravi, Hanzi Mao, Chloe Rolland, Laura Gustafson, Tete Xiao, Spencer Whitehead, Alexander C Berg, Wan-Yen Lo, et al. Segment anything. In *Proceedings of the IEEE/CVF international conference on computer vision*, pages 4015–4026, 2023. 1
- [20] Jingzhi Li, Zongwei Wu, Eduard Zamfir, and Radu Timofte. Recap: Better gaussian relighting with cross-environment captures. In *CVPR*, 2025. 2, 3, 5

- [21] Zhengqi Li, Wenqi Xian, Abe Davis, and Noah Snavely. Crowdsampling the plenoptic function. In *Computer Vision–ECCV 2020: 16th European Conference, Glasgow, UK, August 23–28, 2020, Proceedings, Part I 16*, pages 178–196. Springer, 2020. 3
- [22] Zhihao Liang, Qi Zhang, Ying Feng, Ying Shan, and Kui Jia. Gs-ir: 3d gaussian splatting for inverse rendering. *arXiv preprint arXiv:2311.16473*, 2023. 2, 3, 5, 6, 7
- [23] Yu-Lun Liu, Wei-Sheng Lai, Yu-Sheng Chen, Yi-Lung Kao, Ming-Hsuan Yang, Yung-Yu Chuang, and Jia-Bin Huang. Single-image hdr reconstruction by learning to reverse the camera pipeline. In *Proceedings of the IEEE/CVF conference on computer vision and pattern recognition*, pages 1651–1660, 2020. 4
- [24] Dhruv Mahajan, Ravi Ramamoorthi, and Brian Curless. A theory of spherical harmonic identities for brdf/lighting transfer and image consistency. In *Computer Vision – ECCV 2006*, pages 41–55. Springer, Heidelberg, 2006. 2, 3, 4
- [25] Stephen Robert Marschner. *Inverse rendering for computer graphics*. Cornell University, 1998. 2
- [26] Ricardo Martin-Brualla, Noha Radwan, Mehdi SM Sajjadi, Jonathan T Barron, Alexey Dosovitskiy, and Daniel Duckworth. Nerf in the wild: Neural radiance fields for unconstrained photo collections. In *Proceedings of the IEEE/CVF conference on computer vision and pattern recognition*, pages 7210–7219, 2021. 3
- [27] Ben Mildenhall, Pratul P Srinivasan, Matthew Tancik, Jonathan T Barron, Ravi Ramamoorthi, and Ren Ng. Nerf: Representing scenes as neural radiance fields for view synthesis. *Communications of the ACM*, 65(1):99–106, 2021. 3
- [28] Ravi Ramamoorthi and Pat Hanrahan. A signal-processing framework for inverse rendering. In *Proceedings of the 28th annual conference on Computer graphics and interactive techniques*, pages 117–128, 2001. 2, 4
- [29] Xuqian Ren, Wenjia Wang, Dingding Cai, Tuuli Tuominen, Juho Kannala, and Esa Rahtu. Mushroom: Multi-sensor hybrid room dataset for joint 3d reconstruction and novel view synthesis. In *Proceedings of the IEEE/CVF Winter Conference on Applications of Computer Vision*, pages 4508–4517, 2024. 2, 3
- [30] Shunsuke Saito, Gabriel Schwartz, Tomas Simon, Junxuan Li, and Giljoo Nam. Relightable gaussian codec avatars. In *Proceedings of the IEEE/CVF conference on computer vision and pattern recognition*, pages 130–141, 2024. 2, 3
- [31] Shen Sang and Manmohan Chandraker. Single-shot neural relighting and svbrdf estimation. In *Computer Vision–ECCV 2020: 16th European Conference, Glasgow, UK, August 23–28, 2020, Proceedings, Part XIX 16*, pages 85–101. Springer, 2020. 3
- [32] Pratul P Srinivasan, Boyang Deng, Xiuming Zhang, Matthew Tancik, Ben Mildenhall, and Jonathan T Barron. Nerv: Neural reflectance and visibility fields for relighting and view synthesis. In *Proceedings of the IEEE/CVF conference on computer vision and pattern recognition*, pages 7495–7504, 2021. 3
- [33] Stefan Stojanov, Anh Thai, and James M Rehg. Using shape to categorize: Low-shot learning with an explicit shape bias. In *Proceedings of the IEEE/CVF conference on computer vision and pattern recognition*, pages 1798–1808, 2021. 5, 7
- [34] Cheng Sun, Guangyan Cai, Zhengqin Li, Kai Yan, Cheng Zhang, Carl Marshall, Jia-Bin Huang, Shuang Zhao, and Zhao Dong. Neural-pbir reconstruction of shape, material, and illumination, 2024. 3
- [35] Yao Yao, Jingyang Zhang, Jingbo Liu, Yihang Qu, Tian Fang, David McKinnon, Yanghai Tsin, and Long Quan. Neirlf: Neural incident light field for physically-based material estimation. In *European conference on computer vision*, pages 700–716. Springer, 2022. 3
- [36] Ye Yu and William AP Smith. Inverserendernet: Learning single image inverse rendering. In *Proceedings of the IEEE/CVF Conference on Computer Vision and Pattern Recognition*, pages 3155–3164, 2019. 3
- [37] Jingyang Zhang, Yao Yao, Shiwei Li, Jingbo Liu, Tian Fang, David McKinnon, Yanghai Tsin, and Long Quan. Neirlf++: Inter-reflectable light fields for geometry and material estimation. In *Proceedings of the IEEE/CVF International Conference on Computer Vision*, pages 3601–3610, 2023. 3
- [38] Xiuming Zhang, Pratul P Srinivasan, Boyang Deng, Paul Debevec, William T Freeman, and Jonathan T Barron. Nerfactor: Neural factorization of shape and reflectance under an unknown illumination. *ACM Transactions on Graphics (ToG)*, 40(6):1–18, 2021. 3
- [39] Xiaoming Zhao, Pratul P. Srinivasan, Dor Verbin, Keunhong Park, Ricardo Martin Brualla, and Philipp Henzler. Illuminerf: 3d relighting without inverse rendering, 2024. 3

Supplementary Material for TranSplat

A. Object Segmentation

The full workflow of *TranSplat* includes a segmentation step to extract the Gaussian objects from the source scene. For instance, in main paper Fig. 2 and Fig. 8, we segment the Lego bulldozer from the MipNeRF360 [2] Kitchen scene with our Gaussian segmentation method. We include an additional score variable per 2D Gaussian surfel, quantifying the surfel’s likelihood of belonging to the object of interest. We update these scores during model fitting by propagating information from the 2D input masks to 3D space. After fitting this model, we then simply extract all Gaussians with scores greater than a threshold.

Specifically, following GaussianEditor [8], we equip each Gaussian j with a scalar score w_j computed by:

$$w_j = \frac{\sum_{k=1}^{N_S} \sum_{p=1}^P M^k(p) \cdot \tau_j^k(p)}{\sum_{k=1}^{N_S} \sum_{p=1}^P \mathbb{1}(M^k(p))} \tag{9}$$

where p is a pixel index, $M^k(\cdot)$ is the k -th binary mask (with values of 1 for the object), P is the total number of pixels per image (assuming uniform size), $\mathbb{1}(\cdot)$ is the indicator function, and $\tau_j^k(\cdot)$ is the transmittance function returning a low value for Gaussian j if it has small contribution to rendering pixel p of image k . However, unlike GaussianEditor, we optimize w_j during (instead of after) model fitting, allowing the scores to propagate from parent to children Gaussians in the “densification” process. We find that this strategy is able to capture fine object details not contoured in the initial 2D masks, as fitting progresses (see Fig. 10). We present more semantic segmentation results in Fig. 11.

B. Weighted Sampling for Environment Map to SH Conversion

We estimate SH coefficients for each environment map by sampling their values and performing a least squares fit. We empirically find that a uniform sampling strategy over-represents certain regions of the environment map, leading to tonal inaccuracies during rendering. In particular, consider the differential term $d\omega$ from Eq. 1. In a spherical representation, $d\omega = \sin(\theta) d\theta d\phi$, meaning that light contributions from $\theta \approx 0$ and $\theta \approx \pi$ are far smaller than the contribution from $\theta \approx \pi/2$. To compensate for this disparity, we sample values from an environment map proportional to their $\sin(\theta)$ factors. Fig. 12 demonstrates the advantage of weighted sampling on a simple sphere, rendered in two environments. We used the same number of environment map samples (5000) for both unweighted and weighted cases. Unweighted sampling results in a green hue at the bottom of the sphere, while weighted achieves a result close to ground truth.

C. Ablation on Normal Quality

In Fig. 13, we illustrate the importance of high-quality normals. We chose Gaussian Surfel [9] to fit the training views because each surfel has a well-defined normal. During training, Gaussian Surfel uses normal estimations from OmniData [12] model as priors. Our ablation shows that without this prior, i.e., with less accurate normals, the relighting quality drops significantly.



Figure 10. Example of *TranSplat*’s full pipeline extracting fine details of an object when fitting a GS model to a source scene. *TranSplat* takes input 2D masks, such as the one on the left (generated by SAM [19]), which do not capture fine details such as the flower tendrils. *TranSplat* learns to associate the tendrils with the rest of the vase during optimization due to passing object labels from parent to child Gaussians during densification. The final mask (right) is generated by rasterizing the optimized 3D Gaussian labels into a 2D image.

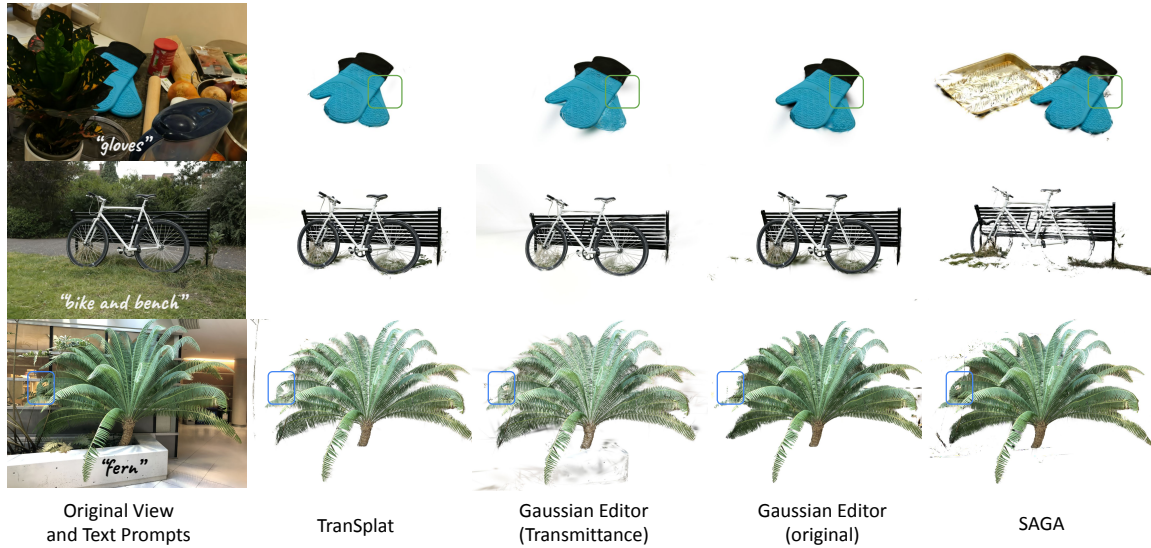


Figure 11. **Object extraction/segmentation results.** This figure presents examples of 3DGS object segmentation, comparing *TranSplat* to two segmentation baselines [7, 8].

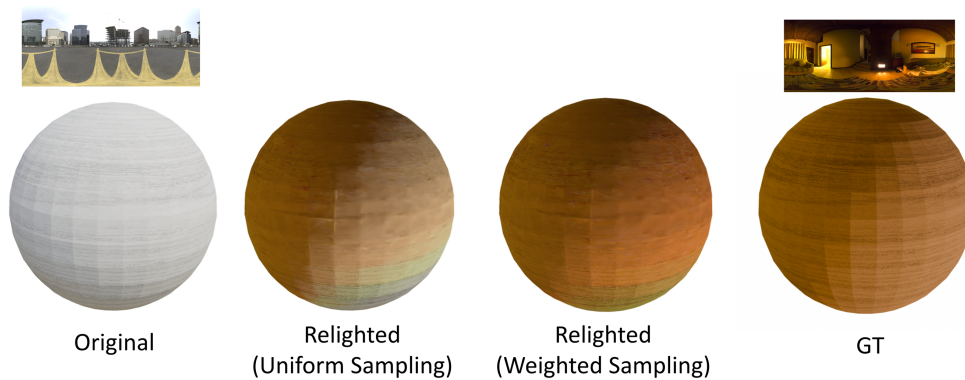


Figure 12. **Experiments on the choice of color sampling method.** The original sphere was under the city environment condition, and we use *TranSplat* to relight it to match the appearance under the fireplace environment. However, uniform sampling leads to inaccuracies when converting the environment map to SH, causing larger color deviations and the appearance of unintended green hues.

D. Scene-Level Relighting

In Fig. 14, we use *TranSplat* to relight two full indoor scenes. We represent the entire scene with GS Surfels [9] for normal estimation. We compare against Recap [20], one of the strongest object-level relighting methods, and *TranSplat* achieves significantly better relighting quality as well as much faster processing speed.

E. Environment Map Visualization

We present additional results of the captured environment maps in Gaussian scenes, including the bicycle, room, and stump scenes from Mip-NeRF 360 [2], two in-house captured scenes used in Fig. 8, and the *vr room* [29] scene used in Fig. 14, as shown in Fig. 15.

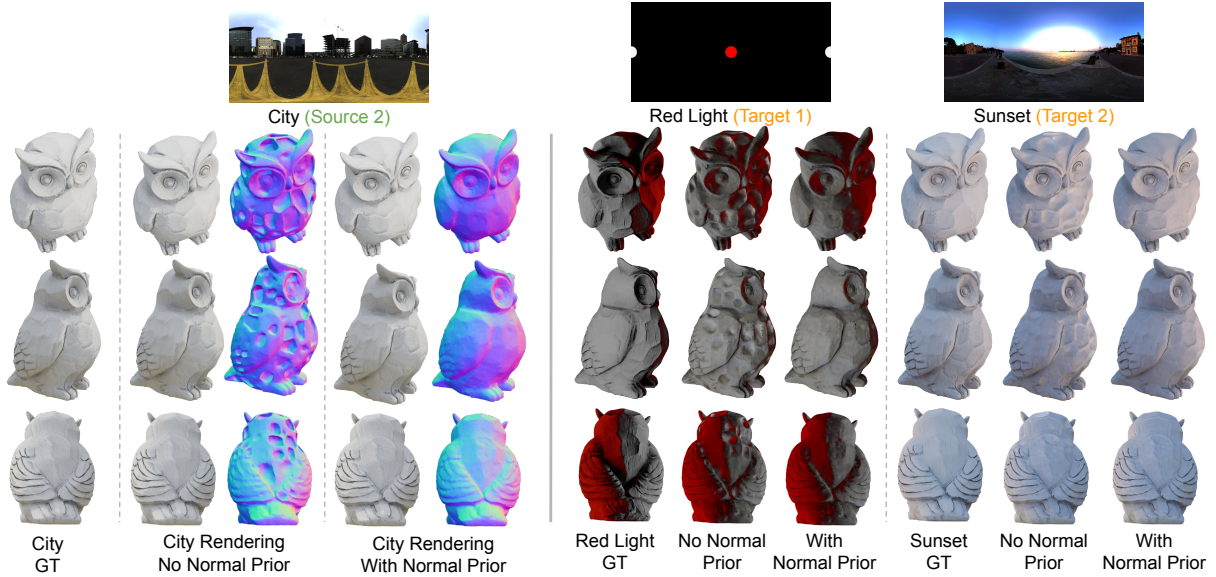


Figure 13. **The effect of normal quality on relighting with *TranSplat*.** Removing the Omnidata [12] normal prior leads to noticeable holes in the predicted surfel object normals. This degradation significantly affects relighting, even though the source renderings are almost identical to the GT.

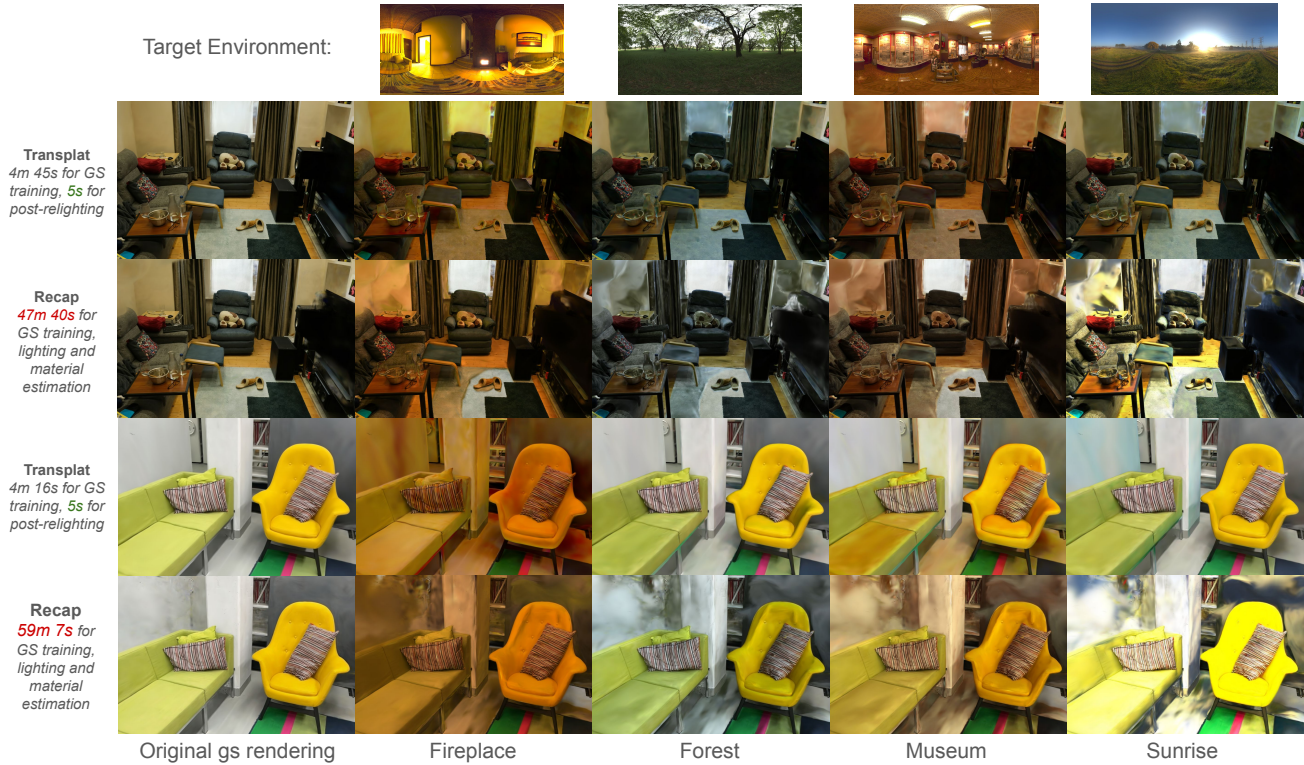


Figure 14. **Experiments on indoor scene relighting.** Although minor artifacts appear due to imperfect normal estimation and complex material properties, *TranSplat* still produces lighting effects that are largely consistent with inverse-rendering-based methods. Moreover, its runtime increases only modestly as the number of Gaussians grows. The two room scenes are from Mip-NeRF360 [2] and MuSHRoom [29] respectively, and the timings are measured on a single RTX 4090.



Figure 15. **Examples of *TranSplat*'s sampled environment maps within the 3DGS scenes.** A cubemap-based capture followed by conversion to an equirectangular map is a straightforward and commonly used approach for generating panoramic images. We novelly apply this directly within a 3D Gaussian Splatting scene, which allows the captured environment map to vary with the sampling location. After converting the map into spherical harmonics, *TranSplat* uses it to relight the object under the position-dependent illumination.

F. Relighting Demonstration Videos

By varying the direction of the environment illumination, we show that the resulting shadows and shading update coherently with the lighting. Please refer to the videos within the supplementary material package.